Acta Crystallographica Section D
Biological Crystallography
ISSN 0907-4449

Structural analysis of human liver glyceraldehyde-3-phosphate dehydrogenase

S. A. Ismail[a,b] and H. W. Park[b]*‡

[a]Department of Molecular Sciences, University of Tennessee Health Science Center, USA, and [b]Department of Structural Biology, St Jude Children's Research Hospital, USA

‡ Present address: Structural Genomics Consortium and Department of Pharmacology, University of Toronto, Canada.

Correspondence e-mail: heewon.park@utoronto.ca

Received 26 May 2005
Accepted 22 August 2005

PDB Reference: human liver glyceraldehyde-3-phosphate dehydrogenase, 1znq, rznqsf.

The crystal structure of human liver glyceraldehyde-3-phosphate dehydrogenase (GAPDH) has been determined. This structure represents the first moderate-resolution (2.5 Å) and crystallographically refined (R_{free} = 22.9%) human GAPDH structure. The liver GAPDH structure consists of a homotetramer, each subunit of which is bound to a nicotinamide adenine dinucleotide (NAD^+) molecule. The GAPDH enzyme has glycolytic and non-glycolytic functions, both of which are of chemotherapeutic interest. The availability of a high-quality human GAPDH structure is a necessity for structure-based drug design. In this study, structural differences between human liver and skeletal muscle GAPDHs are reported in order to understand how these two enzymes might respond to anti-trypanosomatid GAPDH inhibitors.

1. Introduction

Glyceraldehyde-3-phosphate dehydrogenase (GAPDH; EC 1.2.1.12), one of the key enzymes in glycolysis, reversibly catalyzes the first step of the pathway, in which glyceraldehyde-3-phosphate (G3P) is converted into a high-energy phosphate compound, 1,3-bisphosphoglycerate (BPG; Harris & Waters, 1976). The catalytic reaction starts with a nucleophilic attack by the sulfhydryl group of a cysteine from GAPDH on the carbonyl C atom of G3P to form a thiohemiacetal (Harris & Waters, 1976). This reaction is followed by a hydride transfer to nicotinamide adenine dinucleotide (NAD^+) to convert the thiohemiacetal into a high-energy thioester (Harris & Waters, 1976). The high-energy thioester is then attacked by a nucleophilic inorganic phosphate to form the BPG (Harris & Waters, 1976). Two phosphate-binding sites are located within the GAPDH active site and are named the P_i and P_s sites (Moras *et al.*, 1975). The C3 phosphate of G3P binds to the P_i site during the formation of the hemiacetal intermediate and the C3 phosphate then flips from the P_i site to the P_s site before hydride transfer (Skarzynski *et al.*, 1987; Yun *et al.*, 2000).

Tropical protozoan diseases, such as Chagas' disease, leishmaniasis and African trypanosomiasis, are caused by the trypanosomatid parasites *Trypanosoma cruzi*, *Leishmania mexicana* and *T. brucei*, respectively, and result in thousands of deaths every year (http://www.who.org). The bloodstream forms of these trypanosomes depend mainly on glycolysis for ATP production as they do not posses a functional Krebs cycle, making their glycolytic enzymes appealing for structure-based design of selective anti-trypanosomatid drugs (Callens & Hannaert, 1995; Clayton & Michels, 1996; Opperdoes, 1987; Verlinde *et al.*, 1994; Wang, 1995). The glycolytic flux of the bloodstream form of *T. brucei* is mainly controlled by glucose

transporters, followed by aldolase, glycerol-3-phosphate dehydrogenase, GAPDH and phosphoglycerate kinase (Bakker *et al.*, 1997, 1999; Opperdoes, 1987), suggesting that GAPDH is a good target for anti-trypanosomatid drug development. Moderate-resolution GAPDH structures from *T. cruzi*, *L. mexicana* and *T. brucei* are available, as well as a low-resolution structure from human skeletal muscle (Kim *et al.*, 1995; Mercer *et al.*, 1976; Souza *et al.*, 1998; Vellieux *et al.*, 1995). Inhibitors were designed on the basis of the differences between human and trypanosomatid structures in the NAD^+-binding pocket (Verlinde *et al.*, 1994). A high-resolution human GAPDH structure, when available, will provide accurate information on the NAD^+-binding pocket for the design of potent and selective inhibitors.

The non-glycolytic activities of GAPDH have been reported for more than a decade. These activities include nuclear RNA export, phosphotransferase activity, DNA replication and repair, regulation of histone gene expression, nuclear membrane fusion and apoptosis (Sirover, 1999, 2005). The most interesting activity of GAPDH is its role in apoptosis, which has been linked to the translocation and accumulation of GAPDH in the nucleus (Ishitani *et al.*, 1998; Sawa *et al.*, 1997). Recent studies have shown a correlation between apoptosis arising from the accumulation of nuclear GAPDH and several neurodegenerative diseases such as Parkinson's, Alzheimer's and Huntington's diseases (Burke *et al.*, 1996; Kragten *et al.*, 1998; Schulze *et al.*, 1993). Furthermore, the metabolite of the anti-Parkinson drug *R*-(−)-deprenyl (selegiline) [(−)-desmethyl-deprenyl] and its analogue CGP3466 inhibit apoptosis and reduce neuronal and non-neuronal cell death (Carlile *et al.*, 2000; Kragten *et al.*, 1998; Olanow *et al.*, 1995; Patel *et al.*, 1996; Paterson *et al.*, 1997; Tatton *et al.*, 1994; Tatton & Chalmers-Redman, 1996). Evidence suggests that the effects of deprenyl compounds depend on their binding to GAPDH, which in turn interferes with apoptotic signalling pathway and increases neuronal survival (Carlile *et al.*, 2000; Kragten *et al.*, 1998). These findings make GAPDH a promising target for the design of anti-apoptotic molecules that would rescue neural cells from death and prevent the progression of neurodegenerative diseases (Berry, 2004; Reed, 2002). However, the exact GADPH-binding site for these deprenyl compounds is unclear (Berry, 2004; Carlile *et al.*, 2000; Cowan-Jacob *et al.*, 2003; Kragten *et al.*, 1998). Structural insight into the neuroprotective mechanism of deprenyl compounds may provide the key to novel therapeutics for neurodegenerative diseases.

Targeting either the glycolytic or non-glycolytic function of GAPDH is of therapeutic importance and thus the availability of the human GAPDH structure is essential for designing specific and potent drugs. Until now, the human skeletal muscle GAPDH structure, which was solved at 3.5 Å resolution (Mercer *et al.*, 1976), has been the only available human GAPDH structure. In this paper, we describe the first human liver GAPDH structure at 2.5 Å resolution. By comparing the liver and skeletal muscle GAPDH structures we have observed differences that may help explain how these two enzymes respond to a certain class of inhibitors. In addition, this structure may play a role in a structure-based approach for improving the efficiency and safety of deprenyl analogs.

2. Materials and methods

2.1. Protein purification

The cDNA of human liver GADPH (SWISS-PROT Accession No. P04406) was subcloned in pET15b (Novagen), which contains an N-terminal His-tag sequence, and transformed into BL21(DE3) plysS *Escherichia coli* cells (Novagen). Transformants were then allowed to grow at 310 K in LB media to an absorbance of 0.5 at 600 nm. The culture was then induced with a final concentration of 1 m*M* isopropyl β-D-thiogalactopyranoside (IPTG; Anatrace) for 4 h. 4 l bacterial cell culture was harvested by centrifugation at 4000*g* for 15 min and resuspended in 100 ml of a buffer containing 50 m*M* Tris–HCl pH 7.5, 150 m*M* NaCl and 1 m*M* 2-mercaptoethanol. Cells were lysed using a French pressure cell. The lysate was centrifuged at 20 000*g* for 30 min. The supernatant was further filtered through a 0.45 µm cellulose acetate filter. This was followed by an affinity chromatography step in which the crude lysate containing N-terminal hexahistidine-tagged GAPDH was applied onto a Hi-Trap chelating column (Amersham Biosciences) charged with nickel sulfate. GAPDH was eluted using a linear gradient of increasing imidazole concentration. Fractions containing GAPDH were then pooled and the His tag was cleaved by thrombin overnight. The cleaved sample was then subjected to size-exclusion chromatography by loading the sample onto a HiLoad 26/60 Superdex 200 gel-filtration column (Amersham Biosciences) equilibrated with a buffer containing 50 m*M* Tris–HCl pH 7.5, 150 m*M* NaCl, 1 m*M* EDTA and 1 m*M* DTT. Finally, the GAPDH protein was concentrated to 27 mg ml^{-1} with addition of NAD^+ to a final concentration of 0.5 m*M*.

2.2. Crystallization

The initial crystallization condition was obtained from a Nextal screening kit using the hanging-drop vapor-diffusion method. The initial condition was then refined to 0.1 *M* sodium formate and 18%(*w*/*v*) PEG 3350 at 291 K. Plate-shaped crystals appeared after 1 d in the hanging drop, which contained equal volumes of protein and reservoir solutions. Crystals were then flash-frozen in liquid nitrogen using a paraffin:mineral oil mixture (1:1 ratio) as a cryoprotectant.

2.3. Data collection and structure determination

Diffraction data were collected from a flash-frozen crystal at 100 K using a MAR225 CCD detector at the SER-CAT beamline 22-ID at the Advanced Photon Source, Argonne National Laboratory. The data set was indexed and scaled using the programs *DENZO* and *SCALEPACK* (Otwinowski & Minor, 1997). The crystals belong to space group $P2_12_12_1$, with unit-cell parameters a = 124.50, b = 132.31, c = 86.03 Å. The structure was determined by the molecular-replacement method using the program *AMoRe* from the *CCP*4 program suite (Navaza, 1994). One dimer of the rabbit skeletal muscle

GAPDH (PDB code 1j0x; Cowan-Jacob *et al.*, 2003) was used as a search model and two solutions were found by applying rotation and translation functions which correspond to two GAPDH dimers in the asymmetric unit. This homotetramer was then used for rigid-body refinement using the program *CNS* with data between 6.0 and 4.0 Å, which gave an R_{work} of 30%. Simulated annealing was then performed using data between 30 and 2.5 Å and gave an R_{work} of 28%. The $F_o - F_c$ difference map showed electron density corresponding to four NAD^+ molecules (Fig. 1), one per subunit, confirming the correct molecular-replacement solution. Several rounds of refinement using *CNS* and manual fitting of the model to the electron-density map using the program *O* (Jones *et al.*, 1991) were performed. Finally, water molecules were picked using *CNS* and checked manually using *O* (Jones *et al.*, 1991). Non-crystallographic symmetry restraints were applied to the four subunits during the refinement and the final *R* factors of the structure are an R_{work} of 21.09% and an R_{free} of 22.93%. For data-collection and refinement statistics, see Table 1.

Table 1
Data-collection and refinement statistics.

Values in parentheses refer to the highest resolution shell (2.59–2.5 Å).

Data collection	
Radiation source	APS
No. of reflections	
Measured	255331 (8648)
Unique	46609 (3203)
Completeness (%)	91.2 (65.3)
Data redundancy	5.5 (2.7)
R_{sym}† (%)	11.6 (52.3)
Refinement	
Resolution (Å)	30–2.5
R_{work}‡ (%)	21.09 (30)
R_{free}§ (%)	22.93 (31)
No. of protein atoms	10092
No. of ligand atoms	176
No. of water molecules	150
Stereochemistry	
R.m.s.d. bond length (Å)	0.006
R.m.s.d. bond angles (°)	1.3
Average *B* factor (Å^2)	39.6
Residues from Ramachandran plot	
Most favored regions (%)	89.3
General allowed regions (%)	10.0
Generous region (%)	0.3
Disallowed region (%)	0.3

† $R_{sym} = \sum_{h,i} |I_{h,i} - \langle I_h \rangle| / \sum_{h,i} I_{h,i}$. ‡ $R_{work} = \sum ||F_{obs}| - |F_{calc}|| / \sum |F_{obs}|$, where $|F_{obs}|$ and $|F_{calc}|$ are observed and calculated structure-factor amplitudes, respectively. § R_{free} is equivalent to R_{work} except that 5% of the total reflections were set aside for an unbiased test of the progress of the refinement.

3. Results and discussion

3.1. Overall structure

Four subunits designated *O*, *P*, *Q* and *R* with three non-equivalent interfaces (*P*, *Q* and *R*) form the homotetrameric human liver GAPDH, each subunit in which is bound to an NAD^+ molecule (Buehner *et al.*, 1974; Roitel *et al.*, 2003) (Fig. 2). Similar to all other GAPDHs, each subunit consists of an N-terminal NAD^+-binding domain (residues 1–150 and 314–335) and a C-terminal catalytic domain (residues 149–313) (Harris & Waters, 1976) (Fig. 2). The N-terminal NAD^+-binding domain has an α/β dinucleotide-binding fold, while the C-terminal catalytic domain consists of eight-stranded mixed parallel β-sheets connected by either short α-helices or turns (Fig. 2). A Ramachandran plot shows the presence of

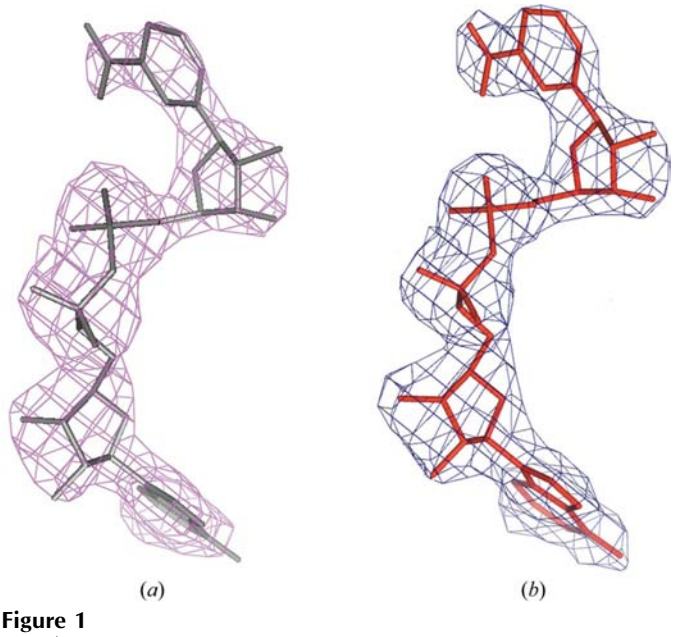

Figure 1
NAD^+ electron-density map. (*a*) Initial $F_o - F_c$ electron density (magenta) of NAD^+ (gray) contoured at 3σ. (*b*) Final $2F_o - F_c$ electron density (blue) of NAD^+ (red) contoured at 1σ. The figure was produced using the program *PyMOL* (DeLano Scientific LLC).

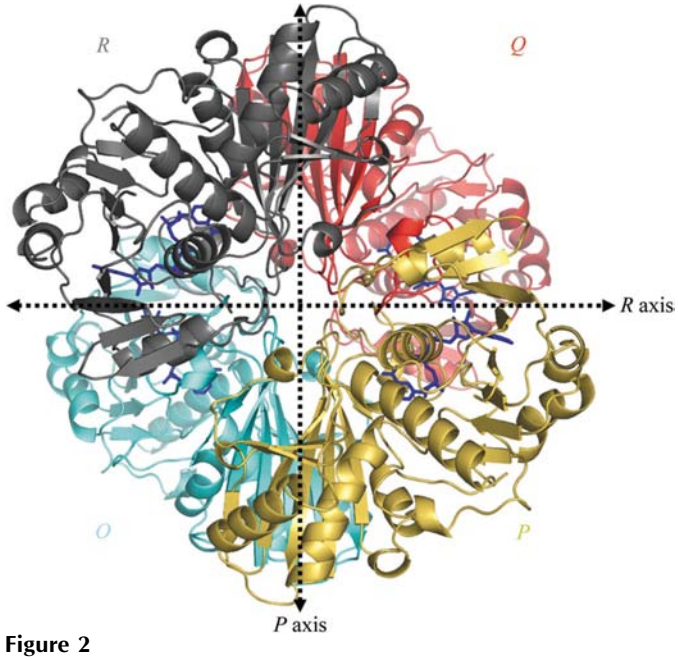

Figure 2
Overall view of the homotetramer of human liver GAPDH. Subunits *O*, *P*, *Q* and *R* are shown in cyan, yellow, red and gray, respectively. Each monomer is bound to an NAD^+ molecule (blue). Symmetry axes are shown as dashed arrows and the *Q* axis is perpendicular to the plane of the paper. This figure was produced using the program *PyMOL* (DeLano Scientific LLC).

Val240 of the four subunits in the most disallowed region, which is characteristic of GAPDH (Kim *et al.*, 1995). In this disallowed conformation, the Val240 main chain forms a hydrogen bond with the side-chain amide of Asn316, which holds Val240 in a position to interact with the nicotinamide ring of NAD^+ as in other GAPDH structures (Souza *et al.*, 1998). An $F_o - F_c$ difference map shows positive density around the active-site cysteine (Cys152) of all four subunits (data not shown). This observation has been reported previously in the rabbit skeletal muscle GAPDH structure and was explained as an oxidation of the cysteine residue to sulfonic acid or *S*-oxy cysteine (Cowan-Jacob *et al.*, 2003).

3.2. Structural comparison with human skeletal muscle GAPDH

The crystal structure of human liver GAPDH is similar to that of the human skeletal muscle GAPDH, with 90% sequence identity and an r.m.s deviation of 1.23 Å for the C^α atoms of the tetramer. In the human liver structure, regions undefined in the human skeletal muscle structure are well defined. These regions include residues 274–304, which are three β-strands connected by loops in the liver structure, whereas in the skeletal muscle structure they appear as a long loop. Also, residues 72–77 and 32–35 are found as two β-strands in the human liver structure which are not well defined in the human skeletal muscle structure. In addition, the Ramachandran plot of the human skeletal muscle structure shows that 8.2% of amino-acid residues are in the disallowed region, which is related to the low resolution (3.5 Å) and twinning of the diffraction data for the human skeletal muscle GAPDH structure (Mercer *et al.*, 1976).

3.3. Structural comparison with rabbit skeletal muscle GAPDH

The structure of human liver GAPDH is very similar to that of rabbit skeletal muscle GAPDH, which was solved at 2.4 Å resolution (Cowan-Jacob *et al.*, 2003), as expected from their high sequence similarity (95%). Superposition of the two tetrameric structures gives an r.m.s deviation of 0.93 Å for C^α atoms. However, there are differences between these two structures. Each subunit of the liver structure is bound to an NAD^+ molecule, while in the rabbit skeletal muscle GAPDH only subunits *P* and *R* were observed to bind NAD^+ (Cowan-Jacob *et al.*, 2003). Subtle conformational changes occur upon NAD^+ binding which bring part of the NAD^+-binding pocket closer to NAD^+. This conformational change is observed in a region comprising residues 78–118 of subunits *O* and *Q*, in which the Ser83 C^α atoms of human liver GAPDH are shifted 2.1 and 3.3 Å, respectively, from the corresponding C^α atoms (Ala80) of rabbit skeletal muscle GAPDH toward bound NAD^+. In addition, a loop containing Gly193 and Lys194 is shifted toward bound NAD^+, which also contributes to the closing of the NAD^+-binding site in human liver GAPDH.

Another difference is the side-chain conformation of Arg234. Two residues, Cys152 and His179, play critical roles in the catalysis mechanism. Cys152 supplies a sulfhydryl group for the nucleophilic attack on G3P, while His179 participates as a base catalyst to facilitate hydride transfer (Soukri *et al.*, 1989; Talfournier *et al.*, 1998; Harris & Waters, 1976). Arg234 is involved in the formation of the P_s site and its chemical modification results in 95% reduction in the GAPDH catalytic rate (Nagradova, 2001; Didierjean *et al.*, 2003; Moras *et al.*, 1975). The conformational switch of the Arg234 side chain has been proposed to play an important role in the regulation of substrate (G3P) binding and product (BPG) release (Souza *et al.*, 1998). This switch mechanism involves either the interactions of Arg234 with Thr182 and Gln185 in the presence of phosphate bound in the P_s site or a salt bridge between Arg234 and Asp198 in the absence of phosphate bound in this site (Souza *et al.*, 1998). In the human liver GAPDH structure, Arg234 stacks with the active-site His179 and interacts with Thr182 and Gln185 (Fig. 3) as if the P_s site were occupied by phosphate; in the human liver structure, however, the P_s site is empty. In contrast, in the rabbit skeletal muscle structure, the side-chain conformation of Arg231 (analogous to Arg234 of human liver GAPDH) points away from the active-site His176 and interacts with Asp195 (Asp198 of human liver GAPDH) as if the P_s site were devoid of phosphate; in the rabbit skeletal muscle structure, however, phosphate is bound in the P_s site (Cowan-Jacob *et al.*, 2003). These observations suggest that the Arg side chain can adopt two different conformations regardless of the phosphate-binding state of the P_s site.

3.4. Implication for trypanosomatid GAPDH-inhibitor design

The overall structure of human liver GAPDH is similar to those of *T. cruzi*, *T. brucei* and *L. mexicana*, with r.m.s deviations of 1.2, 1.5 and 1.4 Å, respectively. Nevertheless, structural differences between human and trypanosomatid GAPDHs in the NAD^+-binding pocket, especially the adenosyl-binding pocket, have been utilized to design selective inhibitors against tyrpanosomatid GAPDHs (Van

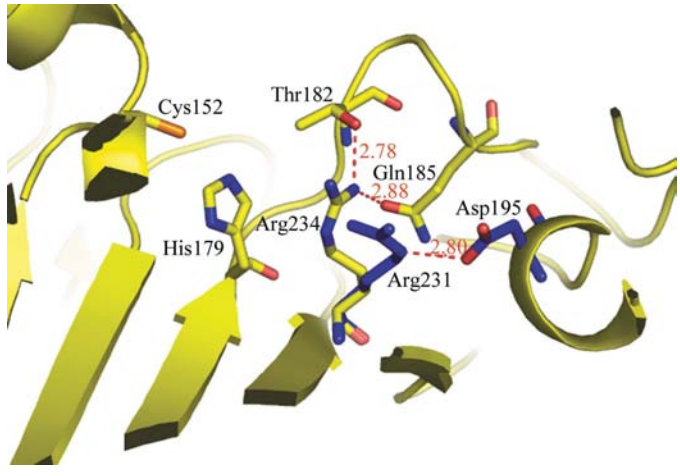

Figure 3
Arg234 conformation. Arg234 of human liver GAPDH (C atoms in yellow) is parallel to His179 and interacts with Thr182 and Gln185, while Arg231 of rabbit skeletal muscle GAPDH (C atoms in blue; PDB code 1j0x) interacts with Asp195 and is perpendicular to His179. The figure was produced using the program *PyMOL* (DeLano Scientific LLC).

Calenberg *et al.*, 1995; Vellieux *et al.*, 1993; Verlinde *et al.*, 1994). Several natural products, including coumarins, have been reported to have significant inhibitory activity towards *T. cruzi* GAPDH (Tomazela *et al.*, 2000). The crystal structure of *T. cruzi* GAPDH bound to chalepin, a coumarin extract from *Pilocarpus spicatus*, shows that the catalytic residue Cys166 and other residues, Thr167, Arg249 and Asp210, interact with the chalepin molecule (Pavao *et al.*, 2002). Several modifications have been proposed to increase the specificity and selectivity of chalepin toward the trypanosomatid GAPDHs (Pavao *et al.*, 2002). One modification was the introduction of a linker arm of one or two C atoms which will bring the chalepin hydroxyl group closer to Asp210 of *T. cruzi* GAPDH for direct hydrogen-bonding interaction (Fig. 4). This exploits the observation that Asp210 of *T. cruzi* is substituted by Leu195 in all human GAPDHs (Pavao *et al.*, 2002). However, in the human liver GAPDH structure, we found that Asp198 could mimic the *T. cruzi* Asp210 interactions with the chalepin hydroxyl group. In contrast, these interactions would not be possible in human skeletal muscle GAPDH since a glycine residue replaces Asp198 of human liver GAPDH. This finding suggests that human liver and human skeletal muscle GAPDHs may respond differently to chalepin-based inhibitors. Since all orally administered drugs are subject to the first-pass effect, liver GAPDH is an important enzyme for consideration in inhibitor design. Therefore, together with the human skeletal muscle GAPDH structure, the human liver GAPDH structure will facilitate the design of more selective inhibitors for *T. cruzi* GAPDH that are non-toxic to humans.

3.5. Implication for apoptotic inhibitor design

R-(−)-Deprenyl (selegiline; DEP) is a drug used in Parkinson's disease and its analogue CGP3466 is in phase II clinical trials for Parkinson's treatment (Berry, 2004; Kragten *et al.*, 1998; Olanow *et al.*, 1995). CGP3466 and the DEP metabolite, (−)-desmethyl-deprenyl, have been reported to bind to GAPDH, block apoptosis and reduce neuronal and non-neuronal death (Carlile *et al.*, 2000; Kragten *et al.*, 1998; Patel *et al.*, 1996; Paterson *et al.*, 1997; Tatton & Chalmers-Redman, 1996). Their ability to reduce neuronal death has been hypothesized to slow the progression of Parkinson's disease (Olanow *et al.*, 1995). A study using neuronally differentiated PC12 cells shows that when they bind to GAPDH, (−)-desmethyl-deprenyl and CGP3466 convert GAPDH from the tetrameric form to a dimer, thereby inhibiting its nuclear accumulation and eventually reducing apoptosis (Carlile *et al.*, 2000). The binding sites of these compounds were suggested to be in a central channel at the interface between the four monomers of GAPDH (Carlile *et al.*, 2000). In another study, rabbit skeletal muscle GAPDH was crystallized in the presence of CGP3466 (Cowan-Jacob *et al.*, 2003). In this rabbit skeletal muscle structure, CGP3466 was not detected in the channel, but at the binding site of the NAD^+ adenine moiety, although the electron density was not unambiguous (Cowan-Jacob *et al.*, 2003). We also tested the effect of (−)-desmethyl-deprenyl on the oligomeric state of human liver GAPDH using an analytical size-exclusion column, but (−)-desmethyl-deprenyl did not convert tetrameric GAPDH to a dimeric form (data not shown). To accurately elucidate the binding site of GAPDH for deprenyl derivatives, we solved the structure of human liver GAPDH crystals soaked with (−)-desmethyl-deprenyl, but (−)-desmethyl-deprenyl could not be seen in the structure (data not shown). As CGP3466 is known to compete with NAD^+ for binding (Kragten *et al.*, 1998), bound NAD^+ at the active site may have prevented (−)-desmethyl-deprenyl from binding to GAPDH. Further studies will be required to visualize the binding site of GAPDH for DEP and its analogues, perhaps by cocrystallizing GAPDH in the presence of excess DEP or its analogues after depleting NAD^+ from the enzyme.

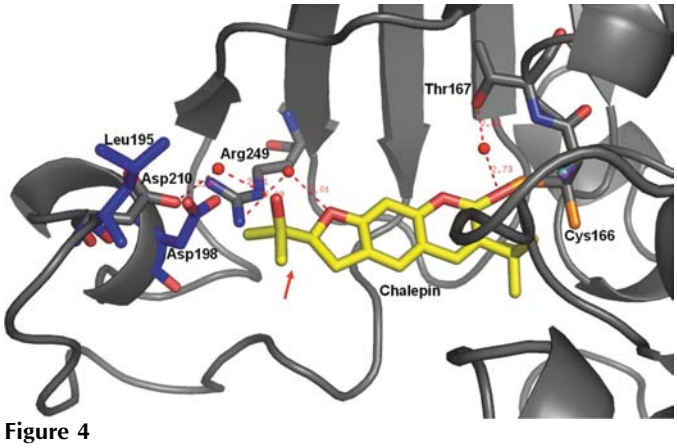

Figure 4
Chalepin-binding site. The binding site of chalepin in *T. cruzi* GAPDH is shown in gray (PDB code 1k3t), whereas Asp198 and Leu195 of human liver GAPDH are in blue. Water molecules involved in the interaction are shown as red dots. The C atoms of chalepin are in yellow. The arrow indicates the region of chalepin proposed for the insertion of an arm linker. The figure was produced using the program *PyMOL* (DeLano Scientific LLC).

4. Conclusion

We have presented the first human liver GAPDH structure at 2.5 Å resolution. Since there is a growing interest in GAPDH as a target for developing chemotherapeutics, structure determination of GAPDH is an essential contribution toward structure-based drug design. In this study, we have also shown the structural differences between the human liver and skeletal muscle GAPDHs, which need to be considered when designing selective inhibitors against trypanosomatid GAPDHs.

We thank Dr William E. Evans for the generous gift of the human liver GAPDH clone and Ms Mikyung Yun for her help in crystal mounting and data collection. This work was supported by grants from St Jude Children's Research Hospital Cancer Centre and American Lebanese–Syrian Associated Charities.

References

Bakker, B. M., Michels, P. A., Opperdoes, F. R. & Westerhoff, H. V. (1997). *J. Biol. Chem.* **272**, 3207–3215.

Bakker, B. M., Walsh, M. C., ter Kuile, B. H., Mensonsides, F. I., Michels, P. A. M., Oppedoes, F. R. & Westerhoff, H. V. (1999). *Proc. Natl Acad. Sci. USA*, **96**, 10098–10103.

Berry, M. D. (2004). *J. Psychiatry Neurosci.* **29**, 337–345.

Buehner, M., Ford, G. C., Moras, D., Olsen, K. W. & Rossmann, M. G. (1974). *J. Mol. Biol.* **82**, 563–585.

Burke, J. R., Enghild, J. J., Martin, M. E., Jou, Y. S., Myers, R. M., Roses, A. D., Vance, J. M. & Strittmatter, W. J. (1996). *Nature Med.* **2**, 347–350.

Callens, M. & Hannaert, V. (1995). *Ann. Trop. Med. Parasitol.* **89** *Suppl.* 1, 23–30.

Carlile, G. W., Chalmers-Redman, R. M., Tatton, N. A., Pong, A., Borden, K. E. & Tatton, W. G. (2000). *Mol. Pharmacol.* **57**, 2–12.

Clayton, C. E. & Michels, P. (1996). *Parasitol. Today*, **12**, 465–471.

Cowan-Jacob, S. W., Kaufmann, M., Anselmo, A. N., Stark, W. & Grutter, M. G. (2003). *Acta Cryst.* D**59**, 2218–2227.

Didierjean, C., Corbier, C., Fatih, M., Favier, F., Boschi-Muller, S., Branlant, G. & Aubry, A. (2003). *J. Biol. Chem.* **278**, 12968–12976.

Harris, J. I. & Waters, M. (1976). *The Enzymes*, 3rd ed., edited by P. D. Boyer, ch. 13. New York: Academic Press.

Ishitani, R., Tanaka, M., Sunaga, K., Katsube, N. & Chuang, D. M. (1998). *Mol. Pharmacol.* **53**, 701–707.

Jones, T. A., Zou, J. Y., Cowan, S. W. & Kjeldgaard, M. (1991). *Acta Cryst.* A**47**, 110–119.

Kim, H., Feil, I. K., Verlinde, C. L., Petra, P. H. & Hol, W. G. (1995). *Biochemistry*, **34**, 14975–14986.

Kragten, E., Lalande, I., Zimmermann, K., Roggo, S., Schindler, P., Muller, D., van Oostrum, J., Waldmeier, P. & Furst, P. (1998). *J. Biol. Chem.* **273**, 5821–5828.

Mercer, W. D., Winn, S. I. & Watson, H. C. (1976). *J. Mol. Biol.* **104**, 277–283.

Moras, D., Olsen, K. W., Sabesan, M. N., Buehner, M., Ford, G. C. & Rossmann, M. G. (1975). *J. Biol. Chem.* **250**, 9137–9162.

Nagradova, N. K. (2001). *Biochemistry (Mosc.)*, **66**, 1067–1076.

Navaza, J. (1994). *Acta Cryst.* A**50**, 157–163.

Olanow, C. W., Hauser, R. A., Gauger, L., Malapira, T., Koller, W., Hubble, J., Bushenbark, K., Lilienfeld, D. & Esterlitz, J. (1995). *Ann. Neurol.* **38**, 771–777.

Opperdoes, F. R. (1987). *Annu. Rev. Microbiol.* **41**, 127–151.

Otwinowski, Z. & Minor, W. (1997). *Methods Enzymol.* **276**, 307–326.

Patel, S. V., Tariot, P. N. & Asnis, J. (1996). *Ann. Clin. Psychiatry*, **8**, 23–26.

Paterson, I. A., Barber, A. J., Gelowitz, D. L. & Voll, C. (1997). *Neurosci. Biobehav. Rev.* **21**, 181–186.

Pavao, F., Castilho, M. S., Pupo, M. T., Dias, R. L., Correa, A. G., Fernandes, J. B., da Silva, M. F., Mafezoli, J., Vieira, P. C. & Oliva, G. (2002). *FEBS Lett.* **520**, 13–17.

Reed, J. C. (2002). *Nature Rev. Drug Discov.* **1**, 111–121.

Roitel, O., Vachette, P., Azza, S. & Branlant, G. (2003). *J. Mol. Biol.* **326**, 1513–1522.

Sawa, A., Khan, A. A., Hester, L. D. & Snyder, S. H. (1997). *Proc. Natl Acad. Sci. USA*, **94**, 11669–11674.

Schulze, H., Schuler, A., Stuber, D., Dobeli, H., Langen, H. & Huber, G. (1993). *J. Neurochem.* **60**, 1915–1922.

Sirover, M. A. (1999). *Biochim. Biophys. Acta*, **1432**, 159–184.

Sirover, M. A. (2005). *J. Cell. Biochem.* **95**, 45–52.

Skarzynski, T., Moody, P. C. & Wonacott, A. J. (1987). *J. Mol. Biol.* **193**, 171–187.

Soukri, A., Mougin, A., Corbier, C., Wonacott, A., Branlant, C. & Branlant, G. (1989). *Biochemistry*, **28**, 2586–2592.

Souza, D. H., Garratt, R. C., Araujo, A. P., Guimaraes, B. G., Jesus, W. D., Michels, P. A., Hannaert, V. & Oliva, G. (1998). *FEBS Lett.* **424**, 131–135.

Talfournier, F., Colloc'h, N., Mornon, J. P. & Branlant, G. (1998). *Eur. J. Biochem.* **252**, 447–457.

Tatton, W. G. & Chalmers-Redman, R. M. (1996). *Neurology*, **47**, S171–S183.

Tatton, W. G., Ju, W. Y., Holland, D. P., Tai, C. & Kwan, M. (1994). *J. Neurochem.* **63**, 1572–1575.

Tomazela, D. M., Pupo, M. T., Passador, E. A., da Silva, M. F., Vieira, P. C., Fernandes, J. B., Fo, E. R., Oliva, G. & Pirani, J. R. (2000). *Phytochemistry*, **55**, 643–651.

Van Calenberg, S., Verlinde, C. L., Soenens, J., De Bruyn, A., Callens, M., Blaton, N. M., Peeters, O. M., Rozenski, J., Hol, W. G. & Herdewijn, P. (1995). *J. Med. Chem.* **38**, 3838–3849.

Vellieux, F. M., Hajdu, J. & Hol, W. G. (1995). *Acta Cryst.* D**51**, 575–589.

Vellieux, F. M., Hajdu, J., Verlinde, C. L., Groendijk, H., Read, R. J., Greenhough, T. J., Campbell, J. W., Kalk, K. H., Littlechild, J. A., Watson, H. C. & Hol, W. G. (1993). *Proc. Natl Acad. Sci. USA*, **90**, 2355–2359.

Verlinde, C. L., Callens, M., Van Calenberg, S., Van Aerschot, A., Herdewijn, P., Hannaert, V., Michels, P. A., Opperdoes, F. R. & Hol, W. G. (1994). *J. Med. Chem.* **37**, 3605–3613.

Wang, C. C. (1995). *Annu. Rev. Pharmacol. Toxicol.* **35**, 93–127.

Yun, M., Park, C. G., Kim, J. Y. & Park, H. W. (2000). *Biochemistry*, **39**, 10702–10710.